Detection of Oriented Repetitive Alternating Patterns in Color Images

A Computational Model of Monkey Grating Cells

Tino Lourens, Hiroshi G. Okuno, and Hiroaki Kitano

Japan Science and Technology Corporation
ERATO, Kitano Symbiotic Systems Project
M. 31 Suite 6A, 6-31-15 Jingumae, Shibuya-ku, Tokyo 150-0001, Japan
{tino, okuno, kitano}@symbio.jst.go.jp

Abstract. In 1992 neurophysiologists [20] found a new type of cells in areas V1 and V2 of the monkey primary visual cortex, which they called grating cells. These cells respond vigorously to a grating pattern of appropriate orientation and periodicity. Three years later a computational model inspired by these findings was published [9]. The study of this paper is to create a grating cell operator that has similar response profiles as monkey grating cells have. Three different databases containing a total of 338 real world images of textures are applied to the new operator to get better a insight to which natural patterns grating cells respond. Based on these images, our findings are that grating cells respond best to repetitive alternating patterns of a specific orientation. These patterns are in common human made structures, like buildings, fabrics, and tiles.

1 Introduction

The accidental discovery of orientation selective cells, which they called *simple* and *complex cells*, in the primary visual cortex by Hubel and Wiesel [5,6] triggered a wave of research activities in neurophysiology. Activities where aimed at a quantitative description of the functional behavior of such cells (e.g., works form De Valois et al. [17,16,1], and von der Heydt [18]). Computational models of simple cells that contain linear filters followed by half-wave rectification are widely accepted, e.g., Movshon [13], Andrews and Pollen [2]. One way of modeling the responses of simple cells is to use Gabor filters [3,7]. Complex cells behave similarly as simple cells, but modeling these cells requires an additional step: spatial summation. Morrone and Burr [12] modeled this summation by taking the amplitude of the complex values of the simple cell operator.

Almost a decade ago, von der Heydt et al. [19,20] reported on the discovery of a new type of neuron in areas V1 and V2 of the monkey visual cortex, they called them *grating cells*, because of their strong responses to grating patterns, but weakly to bars and edges. They estimated that these cells makeup around 4 and 1.6 percent of the population of cells in V1 and V2, respectively, and that around 4 million grating cells of V1 subserve the center 4° of vision. The cells

preferred spatial frequencies between 2.6 and 19 cycles per degree with tuning widths at half-amplitude between 0.4 and 1.4 octaves. They found that the cells are highly orientation selective and that the response is dependent on the number of cycles. A minimum of 2-6 cycles is required to evoke a response and leveled off at 4-14 cycles (median 7.5). In this study we propose a computational model for these grating cells that meet the response profiles of their measurements.

The paper is organized as follows: in Sect. 2 computational models of simple and complex cells are briefly introduced. These models are known from the literature, but since they form part of the grating cells they are included for completeness and clarity. A computational model of grating cells is given in Sect. 3. In the same section we will propose a chromatic sensitive class of grating cells, which is not found (yet) by neurophysiologists, but that is biologically plausible. The chromatic type of cells is based upon the color opponent theory and constructed in analogy with color sensitive orientation selective cells. Section 4 elaborates on the results of the model compared to the measured responses by applying the model to the same test patterns used by von der Heydt et al. In the same section the results of this model are compared with an existing model for grating cells. In Section 5 we apply the model to three databases to get better insights in the response of grating cells to real world images. The last section gives the conclusions.

2 Simple and Complex Cell Operators

The receptive field profiles of simple cells can be modeled by complex-valued Gabor functions:

$$\hat{G}_{\sigma,\lambda,\gamma,\theta}(x,y) = \exp\left(i\frac{\pi x_1}{\sqrt{2}\sigma\lambda}\right)\exp\left(-\frac{x_1^2+\gamma^2 y_1^2}{2\sigma^2}\right) \quad , \tag{1}$$

where $x_1 = x\cos\theta + y\sin\theta$ and $y_1 = y\cos\theta - x\sin\theta$. Parameters σ, λ, γ, and θ represent scale, wavelength ($\frac{2}{\sqrt{2}\sigma\lambda}$ is the spatial frequency), spatial aspect ratio, and orientation, respectively. These Gabor functions have been modified such that their integral vanishes and their one-norm (the integral over the absolute value) becomes independent of σ, resulting in $G_{\sigma,\lambda,\gamma,\theta}(x,y)$, for details we refer to Lourens [11]. They provide a transform of the image $I(x,y)$ via spatial convolution. Afterwards, only the amplitudes of the complex values are retained for further processing:

$$\mathcal{C}_{\sigma,\lambda,\gamma,\theta} = ||I * G_{\sigma,\lambda,\gamma,\theta}|| \quad . \tag{2}$$

This representation, which models the responses of complex cells, is the basis of all subsequent processing. A high value at a certain combination of (x,y) and θ represents evidence for a contour element in the direction orthogonal to θ. Orientations are sampled linearly $\theta_i = \frac{i\cdot 180}{N}, i = 0\ldots N-1$, and the scales are sampled $\sigma_j = \sigma_{j-2} + \sigma_{j-1}$, for $j = 2\ldots S-1$, where σ_0 and σ_1 are known constants.

3 Grating Cells

Von der Heydt et al. [19] proposed a model of grating cells in which the activities of displaced semi-linear units of the simple cell type are combined by a minimum operator to produce grating cell responses. This model responds properly to gratings of appropriate orientation and to single bars and edges. However, the model does not account for correct spatial frequency tuning (the model also responds to all multiples of the preferred frequency).

Kruizinga and Petkov [9,14] proposed a model based on simple cell (with symmetrical receptive fields) input. Responses of simple cells are evaluated along a line segment by a maximum operator M. A quantity q, which is 0 or 1, is used to compensate for contrast differences and a point spread function is used to meet the spatial summing properties with respect to the number of bars and length. Except for the spatial summing properties this model does not meet the other criteria of the grating cells. Also it does not always account for correct spatial frequency tuning; it is unable to discriminate between alternating light and dark bars of preferred frequency and alternating bars of about three times this preferred frequency.

In this paper we propose a grating cell operator that meets both the response profiles of the grating cells and appropriate frequency tuning. This operator uses complex cell input responses, modeled by the operator given in (2). Likewise as in the other models, we evaluate the responses along a line segment perpendicular to the length of the bars of a grating. Unlike the other models, we let the variable length depend on the similarity of the responses of the complex cells, but the length is at least $2B_{\min}$ and at most $2B_{\max}$ bars. Instead of a maximum operator we use an averaging operator. No contrast normalization mechanism is incorporated in the grating operator, since we believe that this is compensated for at the stage of the center-surround cells already, see, e.g., Kaplan and Shapley [8]. This implies that the input data is already normalized for contrast.

3.1 Grating Cell Operator

The initial grating response is calculated as follows:

$$\mathbf{G}^{\text{avg}}_{\sigma,\lambda,\gamma,\theta,l}(x,y) = \frac{\rho}{2l+1} \sum_{i=-l}^{l} \mathcal{C}_{\sigma,\lambda,\gamma,\theta}(x+x_i, y+y_i) \ , \tag{3}$$

where ρ is a response decrease factor. This factor is a measure for the deviation from the optimal frequency and uniformity of the complex cell responses. This factor will be discussed below. Parameter l denotes the length over which summation of the complex cell responses will take place.

The variable length $2l$ over which the responses of the complex cells will be evaluated is between the minimum number of bars $2B_{\min}$ and maximum number of bars $2B_{\max}$. Since the operations are performed on a discrete grid we decompose the maximum length from the center of the line segment, in x- and

y-direction:

$$l_x = \frac{B_{\max}\sqrt{2}\sigma\cos\theta}{\lambda} \quad \text{and} \quad l_y = \frac{B_{\max}\sqrt{2}\sigma\sin\theta}{\lambda} \ . \tag{4}$$

Similarly, we decompose the minimum length ($B_{\min}$) into m_x and m_y. The preferred bar width (in pixels) equals $\sigma\sqrt{2}\lambda$.

Depending on the preferred orientation θ, the evaluation will take place in x- or y-direction. Hence, parameters x_i, y_i, $l_{\min}$ and $l_{\max}$ are orientation dependent:

$$\begin{array}{l} \text{if } \left|\frac{l_y}{l_x}\right| \leq 1 \text{ and } l_x \neq 0 \\ \quad x_i = i;\ \ y_i = \lfloor i\frac{l_y}{l_x} + 0.5\rfloor;\ \ l_{\max} = |\lfloor l_x + 0.5\rfloor|;\ \ l_{\min} = |\lfloor m_x + 0.5\rfloor| \\ \text{else} \\ \quad x_i = \lfloor i\frac{l_x}{l_y} + 0.5\rfloor;\ \ y_i = i;\ \ l_{\max} = |\lfloor l_y + 0.5\rfloor|;\ \ l_{\min} = |\lfloor m_y + 0.5\rfloor| \end{array} \tag{5}$$

where $\lfloor x \rfloor$ denotes the nearest integer value smaller than or equal to x. Length l of (3) is determined by the maximum, minimum, and average response of the complex cells along the line:

$$\begin{array}{l} l = \min_i(l_i), \quad l_{\min} < i \leq l_{\max}, \quad i \in \mathbb{Z} \quad \text{and} \\ \text{if } \frac{\mathbf{G}^{\max}_{\sigma,\lambda,\gamma,\theta,i}(x,y) - \mathbf{G}^{\text{avg}}_{\sigma,\lambda,\gamma,\theta,i}(x,y)}{\mathbf{G}^{\text{avg}}_{\sigma,\lambda,\gamma,\theta,i}(x,y)} \geq \Delta \text{ or } \frac{\mathbf{G}^{\text{avg}}_{\sigma,\lambda,\gamma,\theta,i}(x,y) - \mathbf{G}^{\min}_{\sigma,\lambda,\gamma,\theta,i}(x,y)}{\mathbf{G}^{\text{avg}}_{\sigma,\lambda,\gamma,\theta,i}(x,y)} \geq \Delta \\ \quad l_i = i - 1 \\ \text{else} \\ \quad l_i = l_{\max} \end{array} \tag{6}$$

Constant Δ, which is a uniformity measure, is a value larger than but near 0. We used $\Delta = 0.25$ in all our experiments. The maximum and minimum $\mathbf{G}$ responses are obtained as follows

$$\mathbf{G}^{\Omega}_{\sigma,\lambda,\gamma,\theta,l}(x,y) = \Omega^{l}_{i=-l}\left(\mathcal{C}_{\sigma,\lambda,\gamma,\theta}(x + x_i, y + y_i)\right) \ , \tag{7}$$

where Ω denotes the min or max operator.

The determination of length l depends on the uniformity of responses of the complex cells along a line perpendicular to orientation θ. If the responses of these cells are not uniform enough the summation will be shorter than $l_{\max}$ and consequently the responses will be less strong. We model a linearly increasing response between $B_{\min}$ and $B_{\max}$:

$$\rho_l = \frac{\frac{l}{l_{\max}}B_{\max} - B_{\min}}{B_{\max} - B_{\min}} = \frac{l - l_{\min}}{l_{\max} - l_{\min}} \ . \tag{8}$$

The modeled response also depends on the uniformity of the complex cell responses. Since ρ_l gives a strong decrease for short lengths (it equals 0 for $l_{\min}$), we do not decrease the response for a length between the minimum number of bars and the minimum number plus one:

$$\text{if } (l_s \leq l_{\min}) \quad \rho_u = 1 \quad \text{else} \quad \rho_u = 1 - \frac{\mathbf{G}^{\max}_{\sigma,\lambda,\gamma,\theta,l_s}(x,y) - \mathbf{G}^{\min}_{\sigma,\lambda,\gamma,\theta,l_s}(x,y)}{2\Delta\mathbf{G}^{\text{avg}}_{\sigma,\lambda,\gamma,\theta,l_s}(x,y)} \tag{9}$$

where $l_s = l - \frac{l_{\max}}{1+\lfloor B_{\max} \rfloor}$ is the length that is one bar shorter in length than l. The evaluation on a slightly shorter length ensures that both criteria in (6) are less than Δ, which implies that $\rho_u \geq 0$. Multiplying factors ρ_l and ρ_u results in the response decrease factor $\rho = \rho_l \rho_u$ from (3).

A weighted summation is made to model the spatial summation properties of grating cells with respect to the number of bars and their length and yields the grating cell response:

$$\mathcal{G}_{\sigma,\lambda,\gamma,\theta,\beta} = \mathbf{G}^{\text{avg}}_{\sigma,\lambda,\gamma,\theta,l} * G\text{ß}_{\frac{\sigma\beta}{\lambda}} \ , \tag{10}$$

where Gß is a two-dimensional Gaussian function. In combination with $B_{\min}$ and $B_{\max}$, parameter β determines the size of the area over which summation takes place. Parameters $B_{\min} = 0.5$ and $B_{\max} = 2.5$ together with a β between 2 and 4 yield good approximations of the spatial summation properties of grating cells. In the experiments we used $\beta = 3$.

3.2 Color Opponent Type of Grating Cells

No evidence is given by von der Heydt et al. [20] that there exist color-opponent grating cells. However, it can be made plausible that such type of cells exist. *Opponent* color-sensitive cells are found at the first levels of processing after the photo receptors. Some of them are orientation selective and have an elongated area which give *excitatory* responses to one color and *inhibitory* responses at one or two flanks to another (opposite) color. These opponent color pairs are red-green and blue-yellow or vice versa [10].

Already in the 1960s, Hubel and Wiesel found cells that responded to edges of a specific orientation, but only recently there is evidence that there are cells that are color and orientation selective. Cells of this type are found in area V4 [22] and in area V2 where 21-43% of the neurons have these properties [4,15].

Color-opponent complex cell operators (Würtz and Lourens [21]) are modeled as follows

$$\mathcal{C}^{e,i}_{\sigma,\lambda,\gamma,\theta} = \left| \left| I^e * G_{\sigma,\lambda,\gamma,\theta} - I^i * G_{\sigma,\lambda,\gamma,\theta} \right| \right| \ , \tag{11}$$

where e, i denotes a "red-green" or "blue-yellow" color opponent pair[1] red-green or blue-yellow (yellow=(red+green)/2) and I^a denotes the color channel a from an (r, g, b) image I. In analogy to achromatic grating cell operator of (10), the color-opponent grating cell operator is

$$\mathcal{G}^{\tau}_{\sigma,\lambda,\gamma,\theta,\beta} = \mathbf{G}^{\text{avg},\tau}_{\sigma,\lambda,\gamma,\theta,l} * G\text{ß}_{\frac{\sigma\beta}{\lambda}} \ , \tag{12}$$

where τ is color opponent pair "red-green" or "blue-yellow". The initial grating response from (3) should be modified to

$$\mathbf{G}^{\text{avg},\tau}_{\sigma,\lambda,\gamma,\theta,l}(x,y) = \frac{\rho^{\tau}}{2l^{\tau}+1} \sum_{i=-l^{\tau}}^{l^{\tau}} \mathcal{C}^{\tau}_{\sigma,\lambda,\gamma,\theta}(x+x_i, y+y_i) \ , \tag{13}$$

[1] The order of a color pair is arbitrary since $\mathcal{C}^{e,i}_{\sigma,\lambda,\gamma,\theta} = \mathcal{C}^{i,e}_{\sigma,\lambda,\gamma,\theta}$.

where l^τ and ρ^τ are evaluated as before, but $\mathbf{G}^{\mathrm{avg},\tau}$ should be used instead of $\mathbf{G}^{\mathrm{avg}}$. Similarly, the maximum and minimum $\mathbf{G}$ operators are evaluated by using antagonistic color channels.

The orientations of the grating cells are combined with an amplitude operator (for both $\mathcal{G}$ and $\mathcal{G}^\tau$)

$$\mathcal{G}\mathrm{all}_{\sigma,\lambda,\gamma,\beta} = \sqrt{\sum_{i=0}^{N-1} \left(\mathcal{G}_{\sigma,\lambda,\gamma,\theta_i,\beta}\right)^2} \ , \tag{14}$$

where N denotes the number of orientations and $\theta_i = i\pi/N$. The achromatic and two color opponent (red-green and blue-yellow) channels are combined by taking the amplitudes to yield the final grating operator

$$\mathcal{G}\mathrm{all}_{\sigma,\lambda,\gamma,\beta} = \sqrt{\left(\mathcal{G}_{\sigma,\lambda,\gamma,\beta}\right)^2 + \left(\frac{1}{2}\mathcal{G}^{r,g}_{\sigma,\lambda,\gamma,\beta}\right)^2 + \left(\frac{1}{2}\mathcal{G}^{b,y}_{\sigma,\lambda,\gamma,\beta}\right)^2} \tag{15}$$

at a single scale. Since $\mathcal{C}^{e,i}_\sigma = \mathcal{C}^{i,e}_\sigma$, and hence also $\mathcal{G}^{e,i}_{\sigma,\lambda,\gamma,\theta,\beta} = \mathcal{G}^{i,e}_{\sigma,\lambda,\gamma,\theta,\beta}$, one channel for every opponent pair is sufficient.

4 Properties of Grating Cells

Von der Heydt et al. [20] describe responses to different synthetic grating patterns. In this section the properties of our grating cell operator are evaluated for different settings of parameters λ and γ. The results of this operator for different settings are compared with the measured data and the response properties of the model of Kruizinga and Petkov [9,14].

Von der Heydt et al. performed different tests to obtain the properties of periodic pattern selective cells in the monkey visual cortex. In the first test they revealed the *spatial frequency* and *orientation* tuning of the grating cells. From the second test they obtained the response properties to an increasing number of *cycles* of square-wave gratings. Their third test described the response properties for *checkerboard* patterns by varying the check sizes. The fourth experiment tested the responses to so-called "Stresemann" patterns. These patterns are gratings where every other bar is *displaced* by a fraction of a cycle.

They also tested the responses to contrast. The contrast profiles of the magno and parvo cells [8] show similarities with the profiles given by von der Heydt et al. [20]. In our experiments we will assume that contrast normalization on the input data took place by means of these magno and parvo cells, i.e. contrast normalization is applied to the input image, already. Hence, the test for contrast responses will be omitted in this study.

Von der Heydt et al. also found the so-called *end-stopped grating* cells which respond only at the end of a grating pattern. In this study this type of grating will not be considered.

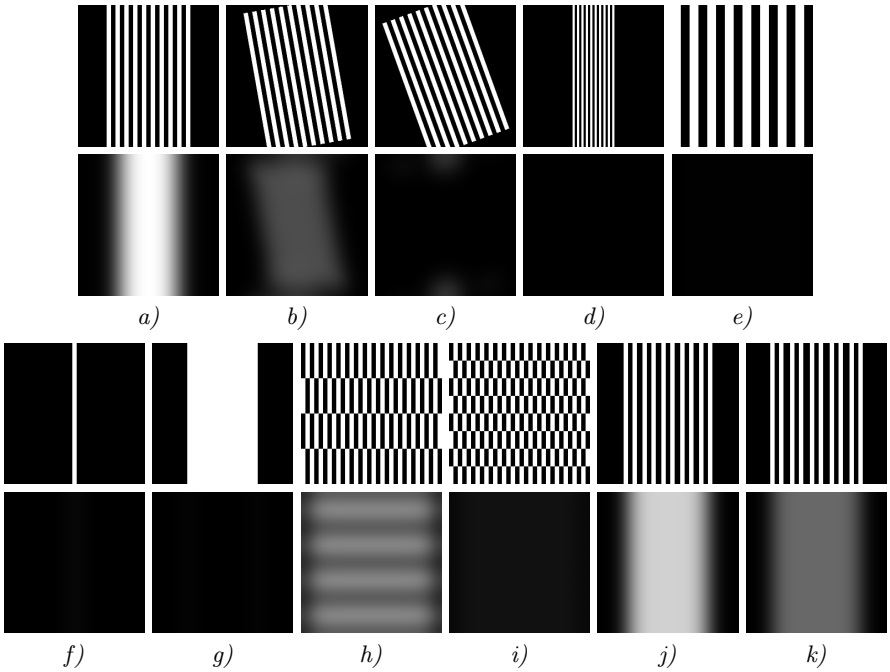

Fig. 1. Responses to square gratings with different orientations and frequencies. Top row gives the stimulus and bottom row the responses of the modeled grating operator. *a)* Grating cells respond vigorously to grating patterns of preferred orientation and frequency. Responses decrease when the pattern differs from this pattern. *b)* and *c)* Responses strongly decrease if the gratings are rotated slightly (10 degrees) and completely vanish at 20 degrees. *d)* and *e)* Doubling or halving the frequency results in zero responses. *f)* and *g)* Grating cells hardly respond to single bars or edges. *h)* and *i)* Increasing the checks in a grating pattern results in a response decrease. *j)* and *k)* Stresemann patterns show similar behavior as in h) and i): the stronger the deviation from a) the weaker its response. The used parameters are $\lambda = 1.00$, $\gamma = 0.25$, $\beta = 3.00$, $B_{\min} = 0.5$, and $B_{\max} = 2.5$.

4.1 Responses to Test Patterns

Figure 1 illustrates that the modeled grating cell operator of (10) shows similar behavior compared to the measurements carried out by von der Heydt et al. [20]. Grating cells respond vigorously to grating patterns of preferred orientation and frequency, but any deviation from this pattern results in a decrease in response.

4.2 Orientation and Frequency Profiles

In this section the properties of grating cells will be modeled as accurate as possible by tuning parameters λ and γ to yield similar responses as measured by von der Heydt et al. [20]. In this paper these profiles are denoted with "vdH ..." in the legends of the figures.

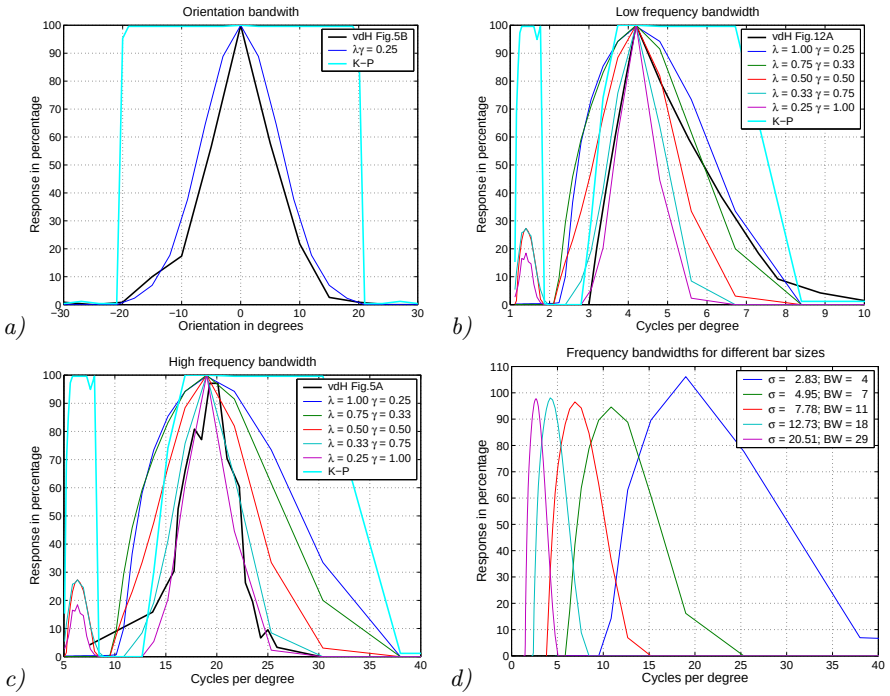

Fig. 2. Measured and modeled response profiles of grating cells. *a)* Orientation, *b)* low frequency, and *c)* high frequency profiles. *d)* Frequency profiles for different preferred bar width sizes (BW = 4, 7, 11, 18, and 29 pixels). Cycles per degree have arbitrary units. Parameters used for d are $\lambda = 1$ and $\gamma = 0.25$.

The orientation bandwidth for grating cells is small, von der Heydt et al. [20] found that the half-maximum responses are at $\pm 6°$. In our model this orientation tuning corresponds approximately to $\lambda\gamma = 0.25$ (Fig. 2a).

Von der Heydt et al. found grating cells with both low and high frequency bandwidth. The response curves of these cells (Fig. 2b and c) are different. Hence, it might be appropriate to model multiple grating cell operators to cover the main bulk of grating cell responses. The modeled grating operators have a smaller bandwidth than the measured grating responses for the low frequency sensitive grating cell, while the same operators (with preferences for higher frequencies) show bandwidths that are similar or slightly larger than the measured responses of grating cells with high frequency preferences. Most appropriate for the low frequency is the model with parameters $\lambda = 1.00$ and $\gamma = 0.25$ while for the high frequency sensitive grating cells $\lambda = 0.33$ and $\gamma = 0.75$ seems a good choice.

However, a problem that occurs for models with γ larger than approximately 0.4 is the response to frequencies that are about a factor 3 larger than the preferred frequency (Fig. 2b and c). If we assume that the preferred bar width is 8 pixels than all bars with a width between 5 and 14 pixels have a response that is stronger than 10 percent of the maximum response ($\lambda = 1$). For $\lambda = 0.33$, bars

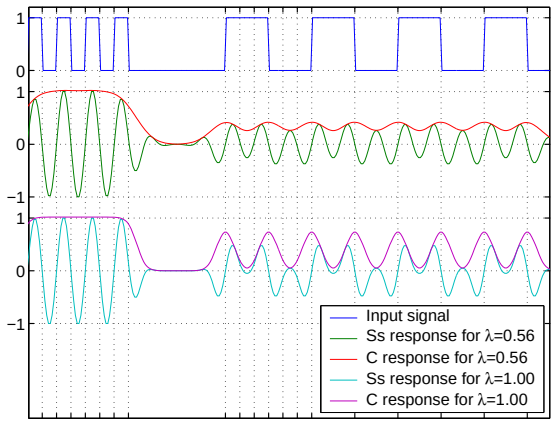

Fig. 3. Input signal (top). Response profile for symmetrical simple and complex cell operators for $\lambda = 0.56$ (middle) and $\lambda = 1.00$ (bottom).

with widths from 6 to 12 and from 20 to 29 pixels have a response stronger than 10 percent of the maximum response. Hence, we suggest to use $\lambda = 1.00$ and $\gamma = 0.25$ for the high frequency sensitive cells also, even though the responses in the second interval never exceed 30 percent of the maximum response.

The frequencies (in cycles per degree) are arbitrary units for the model, since the frequency is determined by the size of the image and the distance of the observer to the image. Hence, modeled grating cells with a preferred bar width of 8 pixels can correspond to both 4.2 and 19 cycles per degree. However, when the preferred bar width is small differences occur in the profile. This is due to the discretization properties of the Gabor filters. Figure 2d illustrates that when the preferred with is 4 pixels the maximum response is over 100 percent. Also, in such case, only 7 measurements can be performed, since it only responds to bars with a width between 1 and 7 pixels.

Figure 2d illustrates the bandwidths for different preferred bar widths, respectively 4, 7, 11, 18, and 29 pixels. The left figure illustrates that these 5 "scales" cover the full range of preferred frequencies (2.6 to 19 cycles per degree) found by von der Heydt et al. If a preferred bar width of 4 pixels is equivalent to 19 cycles per degree than 2.6 cycles per degree corresponds to a bar width of $4 \times 19/2.6 = 29.2$ pixels. The use of these five scales covers the full range well, since the lowest response, between two preferred frequencies, drops at most 25 percent from the maximum response.

The grating cell operator of Kruizinga and Petkov, is available online (`http://www.cs.rug.nl/users/imaging/grcop.html`) and was used with a *bandwidth* of 1.0 and a *periodicity* that equals two times the preferred bar width. The response profile (in our figures denoted by "K-P") of this grating operator shows globally two states: inactive or vigorously firing, which is caused by their normalization quantity q. The choice of $\lambda = 0.56$ gives strong responses to two intervals, which is already caused by the simple cell operators. The interval with

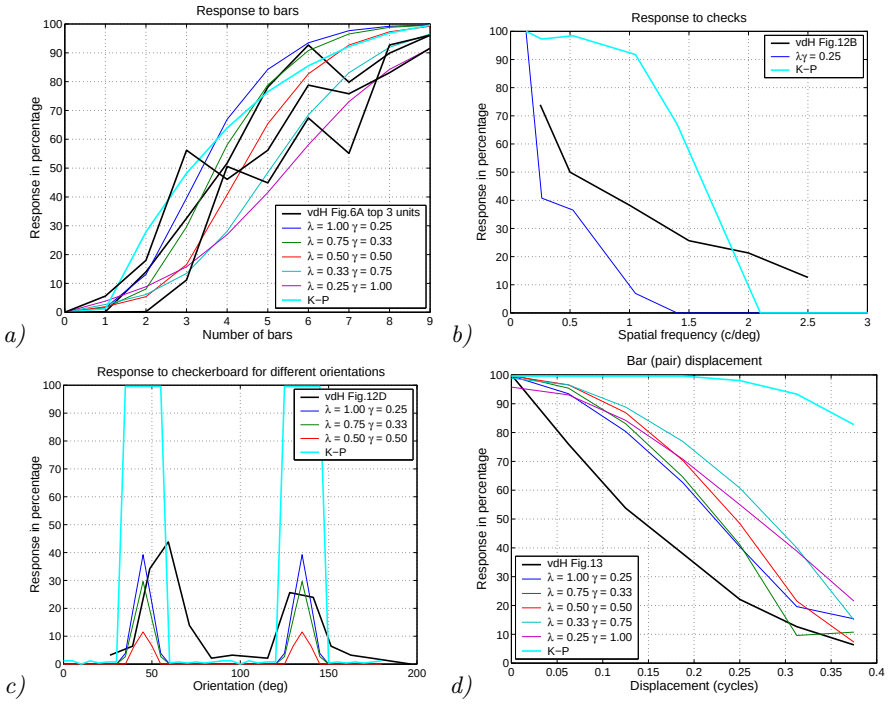

Fig. 4. Measured and modeled properties of grating cells. *a)* Response profile for increasing number of bars. *b)* Response to checks. *c)* Sensitivity to different orientations of a checkerboard pattern. *d)* Responses to increasing shift of a pair of bars, the so-called Stresemann pattern.

the highest frequency (5-11 pixels if the preferred bar width is 8) responds to bars indeed, while the simple cell operator responds to an up and down going edge of a bar in the low frequency interval (19-29 pixels). In the middle of such a low frequency bar there is still some response from both edges, causing a response profile that is similar to that of gratings with preferred frequency. An illustration of this behavior is given for a one-dimensional signal in Fig. 3. This behavior does not occur for $\lambda = 1.00$, as is illustrated in the same figure.

4.3 Profiles for Different Textures

Figure 4a illustrates that the measured results of the grating cells show increasing response with increasing number of bars. In the same figure only one modeled curve is shown, and although modeled grating cells with different parameters show different response curves they all are similar to the responses of the measured cells.

The modeled cells are not as robust to checks as the measured cells as illustrated in Fig. 4b. On the contrary the modeled cells are slightly less sensitive to shifts of bars (Fig. 4d). The responses to different orientations depends on

the orientation bandwidth. If $\lambda\gamma = 0.25$ the orientation bandwidth is similar to that of a measured grating cell, but its response to a checkerboard pattern is low (about three times less) compared to that of the measured grating cells. On the other hand when $\lambda\gamma = 0.35$ the responses are comparable, but in this case the orientation bandwidth is wider than that of the measured cell.

5 Oriented Repetitive Alternating Patterns

It is clear that the model for grating cells responds to grating patterns, but the question that rises is to what kind of real world patterns these cells respond. The latter is important will the operator be successfully applied in an artificial vision system. We used three (Brodatz, ColumbiaUtrecht, and the VisTex) freely available databases containing different textures.

The Brodatz database contains 111 images D1 to D112, where D14 is missing. We cut the central part (512×512 pixels) from the grey scale images that are sized 640×640. The ColumbiaUtrecht database contains 61 images sample01 to sample61. Here we used the central part (256×256 pixels) from the color images that are sized 640×480. In the VisTex database we used 166, 512 square sized color images.

The grating cell operator was applied for $N = 16$ orientations, this number is necessary since the half maximum response of the grating cells is at $\pm 6^\circ$, see also Fig. 2a. We combined all scales with a maximum operator:

$$\mathcal{G}\mathrm{all}_{\lambda,\gamma,\beta} = \max_{i=0}^{S-1} \mathcal{G}\mathrm{all}_{\sigma_i,\lambda,\gamma,\beta}, \tag{16}$$

where $S = 5$ is the number of scales and $\sigma_0 = 4\lambda/\sqrt{2}$, $\sigma_1 = 7\lambda/\sqrt{2}$, and $\sigma_j = \sigma_{j-2} + \sigma_{j-1}$ for $j \geq 2$ (as given earlier). The minimum bar width at σ_0 is 4, since smaller widths lead to strong inaccuracy due to the discreteness of the Gabor filters.

The grating cell operator is very selective and responded in only five (samples 38, 46, 49, 51, and 57) images in the ColumbiaUtrecht database. The operator responded in 32 images of the Brodatz database. In the VisTex database the operator responded to three (buildings, fabric, and tile) out of 18 categories and within the categories it responded to about half of the images.

Based on the results from the three databases we conclude that grating cells respond well to man-made objects that have oriented alternating repetitive patterns. A few of these examples are illustrated in Fig. 5.

6 Conclusions

We presented a new model for grating cells that has similar response profiles as monkey grating cells measured by von der Heydt et al. [20]. Unlike the previous models of grating cells (von der Heydt et al. [19] and Kruizinga-Petkov [9,14]) the new model accounts for proper spatial frequency tuning. The Kruizinga-Petkov model is an oriented texture operator, since it responds well to oriented

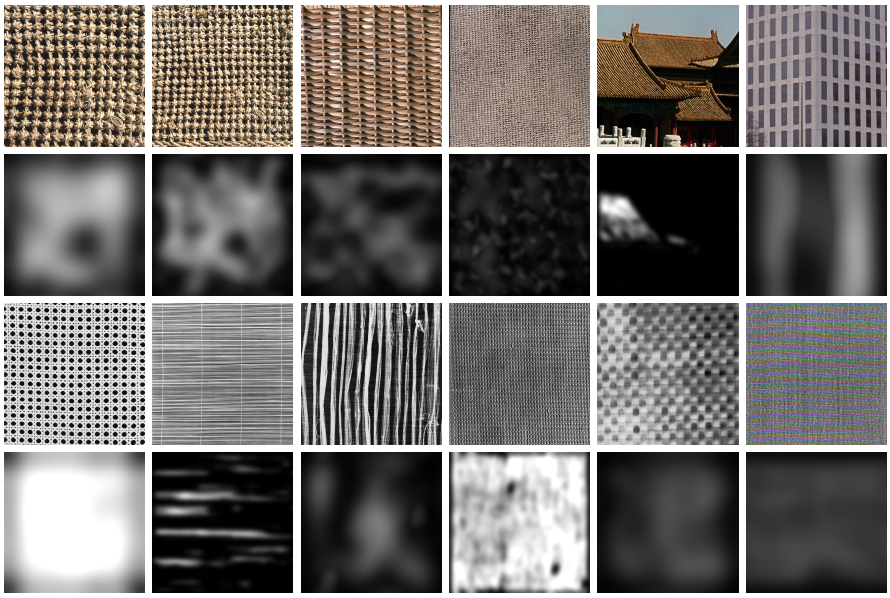

Fig. 5. Images from the databases (odd row) and their response profile (even row) of the grating cells from (16).

texture. Although it is inspired by the work of von der Heydt et al. [20], it is not an accurate model of grating cells because the response profiles differ rather strongly from that of the measured grating cells.

We applied the new model to 338 real world images of textures from three databases. Based upon these results we conclude that grating cells respond to oriented texture, to oriented repetitive alternating patterns to be precise, but are insensitive to many other textures. In general, grating cells are not suitable for texture detection. The grating cell operator responds well if the complex cell responses perpendicular to the preferred orientation show similar strong responses. In such case it is impossible to detect or extract relevant edges in these areas by using complex cells. It therefore seems that grating cells could play a key role in separating form from texture by giving inhibitive feedback responses to the complex cells. A field which we want to explore in the near future.

References

1. D.G. Albrecht, R.L. de Valois, and L.G. Thorell. Visual cortical neurons: are bars or gratings the optimal stimuli? *Science*, 207:88–90, 1980.
2. B. W. Andrews and D. A. Pollen. Relationship between spatial frequency selectivity and receptive field profile of simple cells. *J. Physiol.*, 287:163–176, 1979.
3. John G. Daugman. Uncertainty relation for resolution in space, spatial frequency, and orientation optimized by two-dimensional visual cortical filters. *J. Opt. Soc. Amer.*, 2(7):1160–1169, 1985.

4. K. R. Gegenfurther, D. C. Kiper, and S. B. Fenstemaker. Processing of color, form, and motion in macaque area v2. *Visual Neuroscience*, 13:161–172, 1996.
5. D. Hubel and T. Wiesel. Receptive fields, binocular interaction, and functional architecture in the cat's visual cortex. *Journal of Physiology, London*, 160:106–154, 1962.
6. D.H. Hubel and T.N. Wiesel. Sequence regularity and geometry of orientation columns in the monkey striate cortex. *J. Comp. Neurol.*, 154:106–154, 1974.
7. J. Jones and L. Palmer. An evaluation of the two-dimensional gabor filter model of simple receptive fields in cat striate cortex. *Journal of Neurophysiology*, 58:1233–1258, 1987.
8. E. Kaplan and R. M. Shapley. The primate retina contains two types of ganglion cells, with high and low contrast sensitivity. *Proc. Natl. Acad. Sci. U.S.A.*, 83:2755–2757, April 1986.
9. P. Kruizinga and N. Petkov. A computational model of periodic-pattern-selective cells. In J. Mira and F. Sandoval, editors, *Proceedings of the International Workshop on Artificial Neural Networks, IWANN '95*, volume 930 of *Lecture Notes in Computer Science*, pages 90–99. Springer-Verlag, June 7-9 1995.
10. M. S. Livingstone and D. H. Hubel. Anatomy and physiology of a color system in the primate visual cortex. *J. Neurosci.*, 4:309–356, 1984.
11. T. Lourens. *A Biologically Plausible Model for Corner-based Object Recognition from Color Images*. Shaker Publishing B.V., Maastricht, The Netherlands, March 1998.
12. M. C. Morrone and D. C. Burr. Feature detection in human vision: A phase-dependent energy model. *Proc. of the Royal Society of London*, 235:335–354, 1988.
13. J. A. Movshon, I. D. Thompson, and D. J. Tolhurst. Receptive field organization of complex cells in the cat's striate cortex. *Journal of Physiology*, 283:53–77, 1978.
14. N. Petkov and P. Kruizinga. Computational models of visual neurons specialised in the detection of periodic and aperiodic oriented visual stimuli: bar and grating cells. *Biological Cybernetics*, 76(2):83–96, 1997.
15. H. Tamura, H. Sato, N. Katsuyama, Y. Hata, and T. Tsumoto. Less segregated processing of visual information in v2 than in v1 of the monkey visual cortex. *Eur. J. Neuroscience*, 8:300–309, 1996.
16. K.K. De Valois, R.L. De Valois, and E.W. Yund. Responses of striate cortical cells ito grating and checkerboard patterns. *J. Physiol. (Lond.)*, 291:483–505, 1979.
17. R.L. De Valois, D.G. Albrecht, and L.G. Thorell. Cortical cells: bar and edge detectors, or spatial frequency filters. In S.J. Cool and E.L. Smith III, editors, *Frontiers of Visual Science*, Berlin, Heidelberg, New York, 1978. Springer.
18. R. von der Heydt. Approaches to visual cortical function. In *Reviews of Physiology Biochemistry and Pharmacology*, volume 108, pages 69–150. Springer-Verlag, 1987.
19. Rüdiger von der Heydt, Esther Peterhans, and Max R. Dürsteler. Grating cells in monkey visual cortex: Coding texture? Visual Cortex. In B. Blum, editor, *Channels in the visual nervous system: neurophysiology, psychophysics and models*, pages 53–73, London, 1991. Freund Publishing House Ltd.
20. Rüdiger von der Heydt, Esther Peterhans, and Max R. Dürsteler. Periodic-Pattern-selective Cells in Monkey Visual Cortex. *The Journal of Neuroscience*, 12(4):1416–1434, April 1992.
21. R. P. Würtz and T. Lourens. Corner detection in color images through a multiscale combination of end-stopped cortical cells. *Image and Vision Computing*, 18(6-7):531–541, April 2000.
22. S. Zeki. *A Vision of the Brain*. Blackwell science Ltd., London, 1993.